

A high performance quartz vibrating gyroscope interface circuit driven by square-wave

Qiang Fu, Liang Yin^{a)}, Weiping Chen, Xinpeng Di, Xiaowei Liu, and Wenbo Zhang

MEMS Center, Harbin Institute of Technology,

No. 92, Street Xidazhi, Harbin, China

a) dixinpeng1@163.com

Abstract: A new simple interface circuit for quartz vibrating gyroscope (QVG) driven by square-wave is presented in this paper. The interface circuit is composed of self-excited loop of driving circuit and detecting circuit. Temperature compensation, low noise and low coupling design are adopted in the circuit to achieve the targets of rapid oscillation start, high stability on all-temperature range and linearity. The interface circuit is fabricated in a 0.5 μm CMOS process and the test results show that the scale factor is 19.94 mV/ $^{\circ}$ /s with an input angular ratio range of $\pm 200^{\circ}$ /s. The angular random walk and bias drift are 0.095 $^{\circ}$ / $\sqrt{\text{hr}}$ and 2.5 $^{\circ}$ /hr respectively. The non-linearity can reach to 97 ppm and the zero drift and P-P value are 20 $^{\circ}$ /hr and 80 $^{\circ}$ /hr at the temperature from -45°C to 85 $^{\circ}\text{C}$. Meanwhile, the short stability at room temperature in one hour is 8.86 $^{\circ}$ /hr (1-sigma) and the start time is less than 1 s. This design realizes a high standard with a simple structure.

Keywords: quartz vibrating gyroscope, interface circuit, temperature compensation, high performance

Classification: Integrated circuits

References

- [1] H. Kùlah, *et al.*: “Noise analysis and characterization of a sigma-delta capacitive silicon microaccelerometer,” *IEEE J. Solid-State Circuits* **41** (2006) 352 (DOI: [10.1109/JSSC.2005.863148](https://doi.org/10.1109/JSSC.2005.863148)).
- [2] B. V. Amini, *et al.*: “A 4.5-mW closed-loop micro-gravity CMOS SOI accelerometer,” *IEEE J. Solid-State Circuits* **41** (2006) 2983 (DOI: [10.1109/JSSC.2006.884864](https://doi.org/10.1109/JSSC.2006.884864)).
- [3] M. Yüçetaş, *et al.*: “A high-resolution accelerometer with electrostatic damping and improved supply sensitivity,” *IEEE J. Solid-State Circuits* **47** (2012) 1721 (DOI: [10.1109/JSSC.2012.2191675](https://doi.org/10.1109/JSSC.2012.2191675)).
- [4] O. Oliaei: “Noise analysis of correlated double sampling SC integrators with a hold capacitor,” *IEEE Trans. Circuits Syst.* **50** (2003) 1198 (DOI: [10.1109/TCSI.2003.816314](https://doi.org/10.1109/TCSI.2003.816314)).
- [5] H. L. Xu, *et al.*: “A closed-loop interface for a high-Q micromechanical capacitive accelerometer with 200 ng/Hz input noise density,” *IEEE J. Solid-State Circuits* **50** (2015) 2101 (DOI: [10.1109/JSSC.2015.2428278](https://doi.org/10.1109/JSSC.2015.2428278)).
- [6] V. F. Dias, *et al.*: “Harmonic distortion in SC sigma-delta modulators,” *IEEE*

- Trans. Circuits Syst. I, Fundam. Theory Appl. **41** (1994) 326 (DOI: 10.1109/81.285690).
- [7] Y. F. Dong, *et al.*: “Higher order noise-shaping filters for high-performance micromachined accelerometers,” IEEE Trans. Instrum. Meas. **56** (2007) 1666 (DOI: 10.1109/TIM.2007.904477).
- [8] Y. T. Liu, *et al.*: “A sigma–delta interface ASIC for force-feedback micromachined capacitive accelerometer,” Analog Integrated Circuits Signal Process. **72** (2012) 27 (DOI: 10.1007/s10470-011-9816-1).
- [9] H. Zare-Hoseini, *et al.*: “Modeling of switched-capacitor delta-sigma modulators in SIMULINK,” IEEE Trans. Instrum. Meas. **54** (2005) 1646 (DOI: 10.1109/TIM.2005.851085).
- [10] Y. Zhao, *et al.*: “A $0.57^\circ/\text{h}$ bias instability $0.067^\circ/\sqrt{\text{h}}$ angle random walk MEMS gyroscope with CMOS readout circuit,” IEEE Asian Solid-State Circuits Conference (2015) 9 (DOI: 10.1109/ASSCC.2015.7387505).

1 Introduction

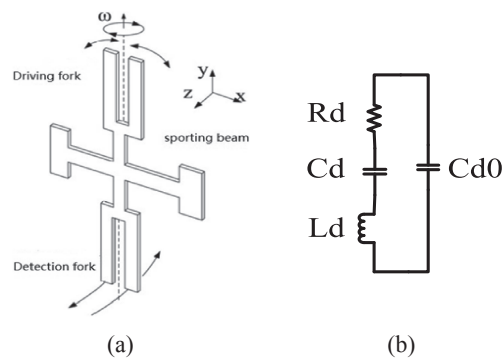


Fig. 1. (a) The quartz element of quartz vibrating gyroscope system.
(b) The electrical equivalent model of QVG

Fig. 1(a) describes the quartz element of quartz vibrating gyroscope system used in this research. The quartz element consists of three parts: a driving fork, a detection fork and a sporting beam. The driving fork is driven by driving force to vibrate in simple harmonic state which is excited by driving force. When there is an angular rate along the driving fork, it will present vibration as a result of Coriolis force. This vibration is at the same frequency with drive signal and its magnitude is proportional to the input angular rate. The vibration can transfer to the detection fork by mechanical coupling. There are charges on the electrode produced by anti-piezoelectric effect of quartz crystal which are then collected by the detection fork. The input angular rate $\Omega \cos \omega t$ can be detected by this process [1, 2, 3, 4, 5, 6]. The electrical equivalent model of QVG can be described as Fig. 1(b).

2 Proposed architecture of interface circuit

Fig. 2 shows interface circuit architecture of QVG self-excited driving loop circuit and detecting circuit. The driven loop is composed of trans-impedance amplifier (E1), peak value detector (E2), PI controller and comparator. Signal which outputs

from driving fork is amplified by trans-impedance amplifier. The amplitude of square-wave driving signal back to driving fork is controlled by an automatic gain control circuit which is adopted to achieve the stable driven to the driving fork. When the driving fork vibrates stable, the amplitude of square-wave driven signal will reach dynamic balance around V_{ref} . The detecting signal flowed from detection fork is sampled and amplified by charge sensing amplifier (E5) and amplifier (E6). Then the signal is demodulated by the signal output from driving circuit (E7) and filtered by a low pass filter (E8). Finally the output of low-pass filter (LPF) and the output of PI controller are set to the input of operational amplifier (E9) which is used to compensate the temperature drift. The overall system is simply to achieve and shows high performance.

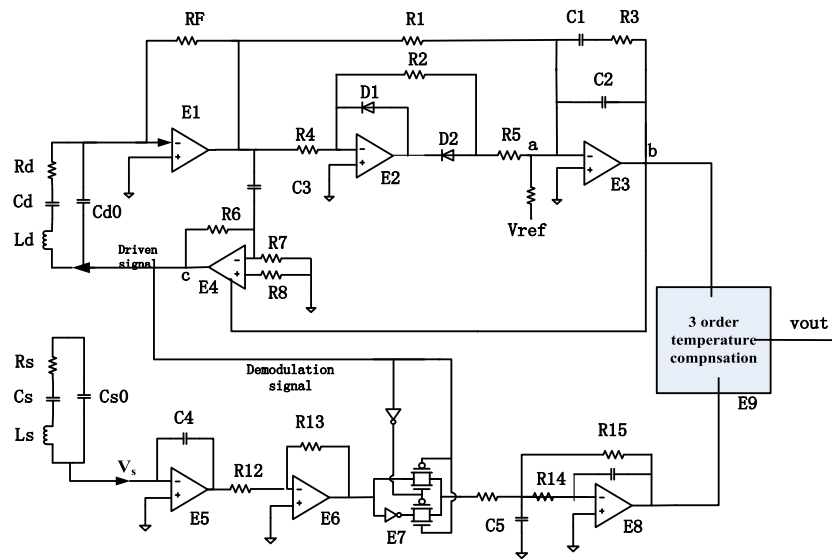


Fig. 2. The interface circuit architecture of QVG

3 Technology realization

To improve the stability of output zero point, three methods are used in the paper. Linking the PI controller output to the low pass filter (LPF) as is shown in Fig. 2 (E8) output by an operational amplifier as is shown in Fig. 2 is to compensate the temperature drift. And a low noise charge sensing amplifier (E5 in Fig. 2) is applied to decrease the output noise. Meanwhile, some other technologies to reduce the coupling are also adopted. And the design based on these technologies above achieves a high stability on all-temperature range, low noise and high linearity interface circuit.

3.1 Temperature compensation

The air damping coefficient is large in QVG since the package of it is usually without high vacuum owing to the high Q value of quartz. In general, the temperature compensation to QVG is designed to use the discrete device which is easier to realize. However, the disadvantages that the temperature can not to be detected on time and the temperature shift unevenly in the QVG will seriously affect the

accuracy of temperature compensation [7]. This paper proposed a new method by connecting the PI controller output to the LPF output by an operational amplifier deal with the temperature compensation.

If $\omega_d = \frac{k_d}{m_d}$, $\varepsilon = \frac{\lambda}{2m_d\omega_d}$, the equation can be rewritten as following:

$$m \frac{d^2x}{dt^2} + 2\varepsilon m\omega_d \frac{dx}{dt} + m\omega_d^2 x = f_d, \quad (1)$$

Which ω_d is the vibrating frequency of driving fork, ε is the damping coefficient. And for the overall system can be driven stability, the driven force f_d should be equal to the damping part expressed as $2\varepsilon m\omega_d \frac{dx}{dt}$, and then: $f_d = 2\varepsilon m\omega_d \frac{dx}{dt}$, ε is the damping coefficient which is linear correlation with the temperature, so it can be given as $\varepsilon(T)$ and f_d is a value linearly depended on T and the temperature drift of output from driving fork can be represented by f_d . The change of driven force f_d which will coupling to the input of charge amplifier in the detecting circuit by the input parasitic capacity gives expression to the output of PI controller, as is shown in Fig. 2, and the coupling signal caused by driven force f_d appears in the output of detecting circuit. Thus the temperature drift can be high-order compensated by making calculation of output of PI controller and output of LPF according to the equation (2):

$$V_{final} = V_{out} + \sum_{i=1}^n k_i V_{dc}^i \quad (2)$$

which V_{final} is the output finally, V_{out} is the output without compensation, V_{dc} is the output of PI controller and k_i is the high-order compensation coefficient. The compensation is operated by computer.

3.2 Low noise design

The noise performance of the detecting circuit is highly depended on the charge sensing amplifier performance and the coupling noise caused by driving circuit. The charge sensing amplifier used in this paper adopted the low noise technique. As is shown in Fig. 3(a), the equivalent noise schematic of precharge amplifier is proposed. The output noise of it can be written as:

$$\begin{aligned} V_{n-out}^2 &= \frac{V_{amplifier}^2 (C_c + C_M + C_P + C_f)^2}{C_f^2} \\ &= \left(\frac{8kT}{3g_{m1}} + \frac{K_f}{WLC_{OX}^2 f} \right) \cdot \frac{(C_c + C_M + C_P + C_f)^2}{C_f^2} \\ &\approx \left(\frac{8kTL}{3\mu_P C_{OX} W (V_{GS} - V_{TH})} + \frac{K_f}{WLC_{OX}^2 f} \right) \cdot \frac{\left(C_c + \frac{2}{3} WLC_{OX} + C_P + C_f \right)^2}{C_f^2} \end{aligned} \quad (3)$$

where C_c is the coupling capacity of the input, C_4 is the feedback capacity, C_p is the parasitic capacitance and C_M is the gate capacity, R_f is the feedback resistance, V_{N-c} is the coupling noise from driving circuit. The coupling capacity C_c is so small that the coupling noise V_{N-c} can be ignored. And the feedback resistance R_f is large enough and the thermal noise can also be neglected. It can be summarized

from the equation (2) that the output noise of charge sensing amplifier will be reduced by minimizing the length of input PMOS pipeline channel. Fig. 3(b) shows the relationship between charge amplifier noise power density and input transistor gate width with different length. The value of width and length are chosen to be $1000\ \mu\text{m}$ and $2\ \mu\text{m}$ according to the curve.

Moreover, the coupling in the input of detecting circuit which is a main reason to generate the temperature drift will be generated due to the usage of square-wave driving signal and the existence of parasitic capacitance of pre-charge amplifier. Meanwhile, the package of the QVG is so small in size that the space-coupling of the input of charge sensing amplifier seriously affects the output of it. In this research, a more stabilized reference voltage V_{ref} is employed to make the output of PI controller stable [8, 9]. Also the low input parasitic capacitance pre-charge amplifier is designed to diminish the coupling caused by layout and taping out. The test results show that the coupling of the detecting circuit satisfies the requirement.

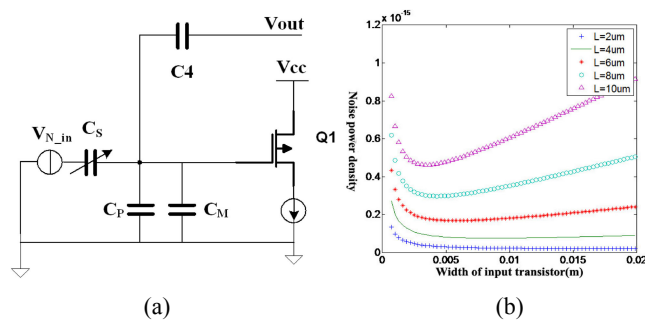


Fig. 3. (a) The equivalent noise schematic of pre-charge amplifier. (b) The relationship between charge amplifier noise power density and input transistor gate width with different length

4 Experimental results

The interface circuit is implemented in a standard $0.5\ \mu\text{m}$ CMOS technology. The test results show the scale factor is $19.94\ \text{mV}/^\circ/\text{s}$ with an input angular ratio range of $\pm 200^\circ/\text{s}$. The allen variance is shown in Fig. 4(a), the angular random walk and bias drift are $0.095^\circ/\sqrt{\text{hr}}$ and $2.5^\circ/\text{hr}$ respectively. The non-linearity is 97 ppm as is shown in Fig. 4(b). The temperature compensation is operated and the sensor is tested at the temperature from -45°C to 85°C . In Fig. 4(c), the result shows the zero drift is $20^\circ/\text{hr}$ and the P-P value is $80^\circ/\text{hr}$. The short stability at room temperature in one hour is $8.86^\circ/\text{hr}$ (1-sigma) as is shown in Fig. 4(d). Because the QVG is driven by square-wave which can drive the driving fork more rapidly than sine-wave, the start time is less than 1 s.

The comparison of this work with QRS11 and QRS116 produced by BEI which is a world's leading cooperation in the QVG interface circuit filed is listed in Table I. Also comparison with Si gyroscope [10] which is published in 2015 with high performance is listed in Table I too. The all temperature stability and non-linearity are highly superior to [10]. Also as known from Table I, the non-linearity of this work exhibits a perfect performance.

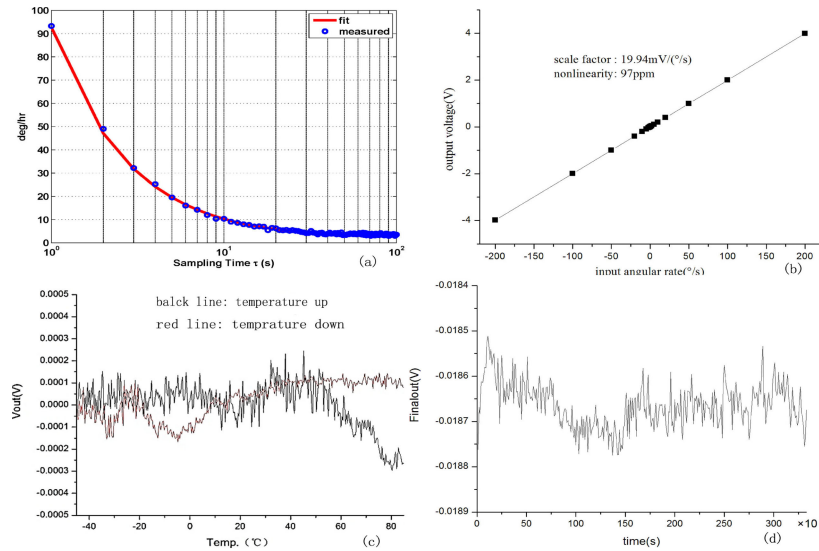


Fig. 4. (a) the curve of allen variance; (b) the curve of linearity; (c) the stability of zero point in all temperature range; (d) stability of sensor in 1 hour.

Table I. Comparison of the this work with reported sensors

Parameter	QRS11	QRS116	[10]	This work
ARW	/	/	$0.067^\circ/\sqrt{\text{hr}}$	$0.095^\circ/\sqrt{\text{hr}}$
Bias Instability	/	/	$0.5^\circ/\text{hr}$	$2.5^\circ/\text{hr}$
Nonlinearity	0.05%	0.05%	/	0.0097%
Short Stability (1-sigma)	$36^\circ/\text{hr}$	$3^\circ/\text{hr}$	$4.9^\circ/\text{hr}$	$8.86^\circ/\text{hr}$
All temperature stability	/	$20^\circ/\text{hr}$	/	$20^\circ/\text{hr}$

5 Conclusions

A new simple interface circuit with rapid oscillation start, high stability and linearity for quartz vibrating gyroscope (QVG) driven by square-wave is presented in this paper. The chip is implemented in a standard $0.5\ \mu\text{m}$ CMOS process. The measurement results show the scale factor is $19.94\ \text{mV}/^\circ/\text{s}$ with an input angular ratio range of $\pm 200^\circ/\text{s}$. The angular random walk and bias drift are $0.095^\circ/\sqrt{\text{hr}}$ and $2.5^\circ/\text{hr}$ respectively. The non-linearity can reach to 97 ppm and the zero drift and P-P value are $20^\circ/\text{hr}$ and $80^\circ/\text{hr}$ at the temperature from -45°C to 85°C . Meanwhile, the short stability at room temperature in one hour is $8.86^\circ/\text{hr}$ (1-sigma) and the start time is less than 1 s. This design realizes a high standard with a simple structure.

Acknowledgments

This work was supported by the National Basic Research Program of China (No. 2012CB934104), National Natural Science Foundation of China (Project 61204121).